

Cobalamin-Dependent and Cobalamin-Independent Methionine Synthases: Are There Two Solutions to the Same Chemical Problem?

by Rowena G. Matthews^{*1}), April E. Smith²), Zhaohui S. Zhou³), Rebecca E. Taurog, Vahe Bandarian⁴),
John C. Evans, and Martha Ludwig

Department of Biological Chemistry, the Biophysics Research Division, and the Life Sciences Institute,
University of Michigan, Ann Arbor, MI 48109-1055, USA

Dedicated to Professor *Duilio Arigoni* on the occasion of his 75th birthday.

*'I find the reaction catalyzed by cobalamin-dependent methionine synthase improbable and that catalyzed by
cobalamin-independent methionine synthase impossible.'*

Duilio Arigoni to Rowena Matthews, Zürich, 1989

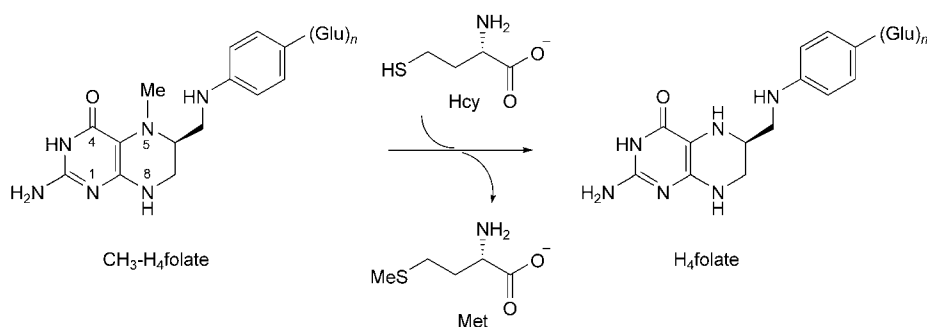
Two enzymes in *Escherichia coli*, cobalamin-independent methionine synthase (MetE) and cobalamin-dependent methionine synthase (MetH), catalyze the conversion of homocysteine (Hcy) to methionine using *N*(5)-methyltetrahydrofolate (CH₃-H₄folate) as the Me donor. Despite the absence of sequence homology, these enzymes employ very similar catalytic strategies. In each case, the p*K*_a for the SH group of Hcy is lowered by coordination to Zn²⁺, which increases the concentration of the reactive thiolate at neutral pH. In each case, activation of CH₃-H₄folate appears to involve protonation at N(5). CH₃-H₄folate remains unprotonated in binary E · CH₃-H₄folate complexes, and protonation occurs only in the ternary E · CH₃-H₄folate · Hcy complex in MetE, or in the ternary E · CH₃-H₄folate · cob(I)alamin complex in MetH. Surprisingly, the similarities are proposed to extend to the structures of these two unrelated enzymes. The structure of a homologue of the Hcy-binding region of MetH, betaine–homocysteine methyltransferase, has been determined. A search of the three-dimensional-structure data base by means of the structure-comparison program DALI indicates similarity of the BHMT structure with that of uroporphyrin decarboxylase (UroD), a homologue of the MT2-A and MT2-M proteins from Archaea, which catalyze Me transfers from methylcorrinoids to coenzyme M and share the Zn-binding scaffold of MetE. Here, we present a model for the Zn binding site of MetE, obtained by grafting the Zn ligands of MT2-A onto the structure of UroD.

Introduction. – The difficult reactions to which *Duilio Arigoni* was referring involve the transfer of a Me group from the tertiary amino group of *N*(5)-methyltetrahydrofolate (CH₃-H₄folate⁵), to the S-atom of homocysteine (Hcy), as shown in

- 1) Correspondence address: 4002 Life Sciences Institute, University of Michigan, 210 Washtenaw Ave., Ann Arbor, MI 48109-2216, USA (phone: +1 734 764 9459; fax: +1 734 763 2492; e-mail: rmatthew@umich.edu)
- 2) Present address: Biology Department, Washington University in St. Louis, Box 1137, St. Louis, MO 63130, USA.
- 3) Present address: Department of Chemistry, Washington State University, Pullman, WA 99164-4630, USA.
- 4) Present address: Department of Biochemistry and Molecular Biophysics, University of Arizona, Tucson, AZ 85721-0088, USA.
- 5) Abbreviations: AcsE, corrinoid iron/sulfur protein methyltransferase (the E subunit of the acetyl CoA synthetase complex); AMT, AcOH/MES/triethanolamine; BHMT, betaine–homocysteine methyltransferase; CH₃-H₄folate, *N*(5)-methyl-5,6,7,8-tetrahydrofolate; CH₃-H₄Pte(Glu)_{*n*}, *N*(5)-methyl-5,6,7,8-tetrahydropteroyl-(poly)glutamate with *n* Glu residues; EDTA, ethylene-1,2-diamine tetraacetate, EXAFS, extended X-ray absorption fine structure; Hcy, homocysteine; H₄folate, 5,6,7,8-tetrahydrofolate; MES, 2-(*N*-morpholino)ethanesulfonic acid; MetE, cobalamin-independent methionine synthase; MetH, cobalamin-dependent methionine synthase; TLCK, *N*_α-tosyl-L-lysine chloromethyl ketone (= *N*-[(1*S*)-5-amino-1-(2-chloroacetyl)pentyl]-4-methylbenzenesulfonamide); *Tris*, tris(hydroxymethyl)aminomethane (= 2-amino-2-(hydroxymethyl)propane-1,3-diol).

Scheme 1. Two Met synthases are known to catalyze this reaction: cobalamin-dependent methionine synthase, the so-called *metH* gene product in *Escherichia coli*, and cobalamin-independent methionine synthase, the *metE* gene product. Homologues of MetH are found in animals, including mammals, and in many species of eubacteria and simple eukaryotes, but not in plants or Archaea. Homologues of MetE are found in plants, insects, yeast, Archaea, and many species of eubacteria, but not in mammals. In the MetE family, Me transfer appears to result from direct attack of Hcy on CH₃-H₄folate⁶⁾; the enzymes do not contain organic prosthetic groups. Me Transfer catalyzed by MetH involves the cobalamin prosthetic group, and transfer occurs from methylcobalamin to Hcy, leading to methionine and cob(I)alamin, and then from CH₃-H₄folate to cob(I)alamin to regenerate the methylcobalamin cofactor and form H₄folate.

Scheme 1. *Reaction Catalyzed by Methionine Synthases.* The MetE enzyme appears to catalyze a direct attack of the S-atom of Hcy on the N(5) Me group of CH₃-H₄folate, while methyl transfer catalyzed by MetH involves the cobalamin cofactor as an intermediary. MetH can use substrates with one or more Glu residues ($n \geq 1$), while MetE requires at least three Glu residues ($n \geq 3$).



Tertiary amines are not good Me donors; the pK_a of the corresponding H₄folate anionic leaving group is estimated to be > 30 . The available evidence suggests that activation of CH₃-H₄folate occurs by protonation at N(5); in solution, the pK_a of the resulting ammonium compound is 5.05 [1]. Thus, at physiological pH, only *ca.* one molecule in 100 is in the correct protonation state for reaction. The microscopic pK_a of the SH group of Hcy is 10 [2], and the thiol as such is not nucleophilic. Thus, only one in 1000 molecules of Hcy will be in the reactive thiolate form at neutral pH.

A further complication is that, in aqueous solution, protonated CH₃-H₄folate would react with the Hcy thiolate by H⁺ transfer rather than by group transfer. This is avoided in 'improbable' MetH by the interposition of the cobalamin cofactor in the Me-transfer sequence, *i.e.*, CH₃-H₄folate and Hcy do not contact one another in the course of the reaction. But in the 'impossible' reaction catalyzed by MetE, H⁺ transfer between substrates must be avoided. A simple solution to this catalytic dilemma would be for the enzymes to lower the pK_a of Hcy below 7, while raising the pK_a of CH₃-H₄folate above 7, maximizing the concentration of the reactive forms of the substrates and minimizing

⁶⁾ MetE requires three or more Glu residues in its CH₃-H₄folate substrate (CH₃-H₄Pte(Glu)_{*n*}) for efficient catalysis, while MetH can use CH₃-H₄folate substrates with one or more Glu residues. The Glu residues in CH₃-H₄Pte(Glu)_{*n*} are connected by amide linkages involving the γ -carboxylate of the preceding residue.

H⁺ transfer between protonated CH₃-H₄folate and Hcy. Here, we provide evidence consistent with this hypothesis and discuss the molecular strategies by which the pK_a of Hcy is decreased.

Faced with these formidable chemical challenges, it is also of interest to know the degree to which the catalytic strategies available to MetE and MetH are constrained. While both MetE and MetH are present in *Escherichia coli*, they do not show any detectable sequence homology. How do two apparently unrelated enzymes accomplish this challenging chemical reaction: do they employ similar or different strategies for catalysis?

Strategies for Homocysteine Activation. – The initial insight into the catalytic strategy for MetE came with the observation that the enzyme was inactivated when TLCK⁵, included in the buffers used for the purification of MetE, reacts with Cys⁷²⁶, an absolutely conserved residue in the amino acid sequences of the MetE family [3]. A Cys⁷²⁶Ser mutant was devoid of catalytic activity. Essential cysteine residues typically function as nucleophiles in redox reactions or as metal ligands. Wild-type MetE was found to contain 1.02 equiv. of Zn, while the isolated mutant enzyme was Zn-free [4]. Removal of Zn from the wild-type enzyme by treatment with urea and EDTA resulted in loss of activity, and activity was restored upon adding Zn. Extended X-ray-absorption fine-structure analysis (EXAFS) indicated that the Zn was ligated by two O- or N- and by two S-atoms [4]. Consistent with binding of the SH group of homocysteine directly to Zn, addition of Hcy was shown to result in a change in coordination to ligation by one O- or N-ligand and three S-ligands. Taken together, these results suggested that Zn acts as a *Lewis* acid catalyst, lowering the pK_a of the SH group of Hcy. The proposed interaction of Hcy with Zn was confirmed by use of L-selenohomocysteine [5] and EXAFS measurements at the Se and Zn edges to demonstrate Se coordination to Zn and *vice versa* [6].

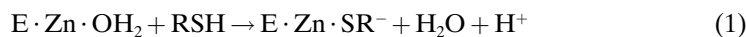
Alignment of the sequences of MetE homologues from eubacteria, eukaryotes, and Archaea indicated that only three residues are absolutely conserved. Besides Cys⁷²⁶, the invariant residues are His⁶⁴¹ and Cys⁶⁴³. His⁶⁴¹Gln and Cys⁶⁴³Ser mutants show decreased affinity for zinc and greatly reduced the activity, consistent with their role as Zn ligands [7]. The fourth ligand to Zn in the resting enzyme is assumed to be H₂O, which is displaced on addition of Hcy. Released protons on binding of Hcy to MetE can be detected by titrations of the enzyme with Hcy in a weakly buffered solution containing phenol red as a pH indicator. Addition of Hcy to MetE results in proton release (0.85 equiv. per mol of MetE at an initial pH of 7.6), consistent with displacement of a neutral H₂O molecule by the sulfido (S⁻) anion⁷⁾.

Despite the lack of similarity between the MetH and MetE sequences, their strategies for Hcy activation both involve Zn as a *Lewis* acid. Dissection of the 1,227-residue polypeptide of MetH from *E. coli* revealed that the region responsible for the binding of Hcy was contained in the first 353 amino acids. The truncated polypeptide MetH⁽²⁻³⁵³⁾ could be expressed and was shown to catalyze Me transfer from exogenous methylcobalamin to Hcy [8]. This module shows significant sequence homology with

7) Z. S. Zhou, R. G. Matthews, unpublished results.

betaine–homocysteine methyltransferase (BHMT), an enzyme that transfers Me groups from the quaternary amine betaine to homocysteine. Both the Hcy-binding module of MetH and BHMT contain invariant vicinal cysteines [9], Cys³¹⁰ and Cys³¹¹ in the sequence of MetH (*E. coli*), and mutation of these Cys residues to Ala results in loss of methylcobalamin–Hcy methyltransferase activity [8]. Indeed, MetH was shown to contain stoichiometric amounts of Zn, and Cys³¹⁰Ala or Cys³¹¹Ala mutants were shown to lack Zn [10]. EXAFS Studies revealed that the wild-type enzyme, when isolated, contains three S-ligands and one N- or O-ligand (presumably H₂O) to the Zn ion. Addition of Hcy then results in an altered EXAFS spectrum consistent with Zn ligation by four S-ligands [11]. A third invariant Cys was identified in homologues of MetH, and the Cys²⁴⁷Ala mutant was shown to lack both methylcobalamin–Hcy methyltransferase activity and Zn. Later on, BHMT was shown to require Zn as well [12].

Using phenol red as an indicator in experiments conducted in 50- μ M potassium phosphate buffer/100-mM KCl, binding of Hcy to MetH was accompanied by the release of a proton (0.9 H⁺ per equiv. of MetH) at pH 7.8, consistent with binding of Hcy as the thiolate anion and with the role of Zn as a *Lewis* acid catalyst [13]. Conversion of a thiol to a Zn-bound thiolate is associated with an increase in the far-UV absorbance due to ligand–metal charge transfer [14]. The wavelength maximum and molar absorptivity of the charge-transfer complex varies with the metal and the ligands, and the molar absorptivity changes (based on Zn) at 236 nm range from 5,000 to 15,000 M⁻¹cm⁻¹ for ligation of sulfido groups to Zn [14][15]. The wavelength maximum for the lowest-energy charge-transfer band is sensitive to the electro-negativity of the ligand and the metal; for Zn–thiolate complexes, it lies at *ca.* 235 nm. When a fourth ligand is added to a complex containing three pre-existing ligands, the wavelength and the molar absorptivity of the difference spectrum may vary with the nature of the ligands. The combined absorbance of cobalamin and the protein obscures this region of the spectrum in MetH, but the binding of Hcy can be monitored in an N-terminal fragment MetH^(2–649), containing the Hcy-binding and folate-binding regions of the enzyme, but lacking the cobalamin-binding region. This fragment retains the ability to catalyze Me transfers from CH₃-H₄folate to exogenous cob(I)alamin, and from exogenous methylcobalamin to Hcy [8]. *Figs. 1,a* and *1,b* show a titration of MetH^(2–649) with Hcy conducted at pH 8.5, where the binding of Hcy to MetH^(2–649) is nearly stoichiometric. The maximum change in molar absorptivity at $\lambda_{\text{max}} = 236$ nm was calculated to be 8,330 M⁻¹cm⁻¹, which is within the range of the previously reported values. These titrations clearly indicate that Hcy is bound as the thiolate at pH 8.5. Experiments were conducted in three different buffer systems, and the maximum change in absorbance at 236, measured at high pH, was approximately the same in each buffer system. The pH dependence of Hcy binding determined in this manner is shown in *Fig. 1,c*. Above *ca.* pH 7.5, *K_d* for homocysteine binding does not vary with pH, while, below this pH, it increases *ca.* 10-fold for each unit decrease in pH. Since the absorbance changes at 236 nm at saturating Hcy concentration do not change with pH, we know that Hcy binds as the thiolate throughout the stability range of the enzyme (*E*). The increase in the measured *K_d* at low pH is consistent with:



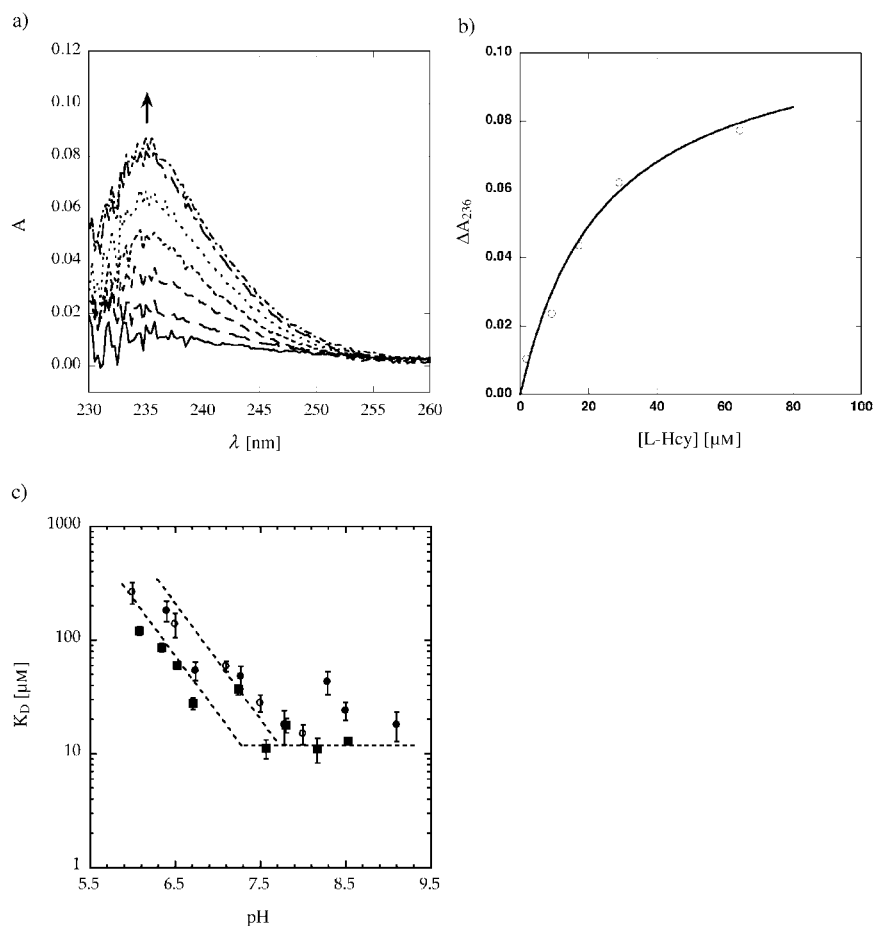


Fig. 1. UV/VIS Spectra, Titration Curve, and pH Dependence of K_D for the Formation of a Zn–Thiolate Complex in $\text{Meth}^{(2-649)}$ in the Presence of L-Hcy. The formation of a charge-transfer band ($\lambda = 236$ nm) was monitored in the presence of increasing concentrations of L-Hcy in three buffer systems. A representative set of a) UV/VIS spectra (recorded in AcOH/MES/Tris buffer, pH 8.5) and b) the resulting titration curve are shown. The concentration of $\text{Meth}^{(2-649)}$ was $25 \mu\text{M}$, and the calculated molar absorbance change at 236 nm was $8,830 \text{ M}^{-1}\text{cm}^{-1}$. The calculated K_D values from three sets of studies, each performed in a different buffer system, are shown in c). The buffers contained 25-mM AcOH, 25-mM MES, 50-mM Tris (■); 20-mM AcOH, 20-mM MES, 40-mM *N*-ethylmorpholine (○); or 20-mM MES, 20-mM *N*-ethylmorpholine, 40-mM ethanolamine (●). The dashed lines in the ascending portions of the pH profile are calculated for the release of 1 equiv. of H^+ per equiv. of L-Hcy bound. Two ascending dashed lines are shown, one fit to the data obtained from titrations in AcOH/MES/Tris buffer, and one fit to the data obtained in the other two buffer systems. For abbreviations, see footnote 5.

Above pH 7.5, the binding of Hcy becomes pH-independent, which indicates that net proton release is no longer associated with binding. Hcy has no $\text{p}K_a$ values in this region (the $\text{p}K_a$ values for the ammonium group and the SH group are > 9), so the stoichiometry indicates that a group on the free enzyme has become deprotonated in

this range. The most-plausible assumption is that the Zn-bound H₂O molecule undergoes ionization⁸⁾ above pH 7, *i.e.*:

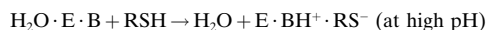


There are some hints that the measured K_a values and the apparent pK_a for the Zn-bound H₂O vary with the composition of the buffer, which perhaps explains why nearly stoichiometric H⁺ release was observed at pH 7.8 (phenol red experiments) while measurements made in acetate/MES/*Tris* buffer predict substoichiometric H⁺ release at this pH. Despite these uncertainties, the measurements tell us that the pK_a of the SH group of Hcy bound to the Zn-atom of MetH must be less than 6, so that, at neutral pH, bound homocysteine is almost completely in the reactive thiolate form.

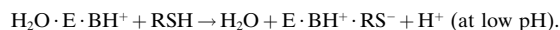
Thus, the chemical strategies for Hcy activation in MetE and MetH are remarkably congruent: Zn is used as a *Lewis* acid catalyst to lower the pK_a of bound Hcy, so that the thiolate is the dominant form at neutral pH. Despite these similarities, the ligands used to coordinate Zn are different: MetE employs a His-X-Cys motif and a downstream Cys, whereas MetH uses an upstream Cys and a downstream Cys-Cys motif for Zn coordination. Furthermore, the net charge on the Hcy-bound MetH Zn center should be -2 , assuming that all four ligands are thiolates, while the net charge on the Hcy-bound MetE center is presumably -1 , assuming that the His ligand is neutral and the remaining ligands are thiolates. Model studies on the reactivity of Zn tetrathiolates and compounds in which one or more thiolates are replaced by imidazole indicate that reduction of the net charge at the Zn center results in decreased reactivity [16].

Strategies for Methyltetrahydrofolate Activation. – *Binary Complex Formation Is not Associated with Protonation.* One might have expected MetE and MetH to stabilize a protonated form of bound CH₃-H₄folate, but this does not appear to be the case. The UV/VIS absorbance spectrum of free CH₃-H₄folate is pH dependent, and protonation at N(5) is associated with a decreased absorbance at *ca.* 300 nm and an increased absorbance at 265 nm, as shown by the dashed line in Fig. 2 [1]. Such changes would be obscured by the absorbance of the cobalamin cofactor in MetH, but are easily detected in the truncated fragment MetH⁽²⁻⁶⁴⁹⁾. Titration of MetH⁽²⁻⁶⁴⁹⁾ with CH₃-H₄folate induces an increase at 308 nm and a decrease at 265 nm in the UV spectrum; these spectral changes are not consistent with protonation of CH₃-H₄folate. The observed red shift probably reflects the introduction of CH₃-H₄folate into a hydrophobic environment [1]. Similar changes are observed throughout the pH range from 9.3 to 5.3, suggesting a pK_a below 5 for protonation of N(5) of CH₃-H₄folate in the binary complex.

⁸⁾ We cannot exclude the possibility that the inflection seen in Fig. 1.c results from the deprotonation of a residue on the enzyme, as discussed by *Rozema* and *Poulter* [15]. They proposed that binding of SH-containing peptides to protein farnesyl transferase occurs with the following stoichiometries:



or



However, the structure of betaine-homocysteine methyl transferase with Hcy bound at the active site does not reveal any candidates for a base with a pK_a that would be dependent on whether or not Hcy is bound to Zn. The carboxylate group of Hcy is H-bonded to backbone amide rather than to protein side chains.

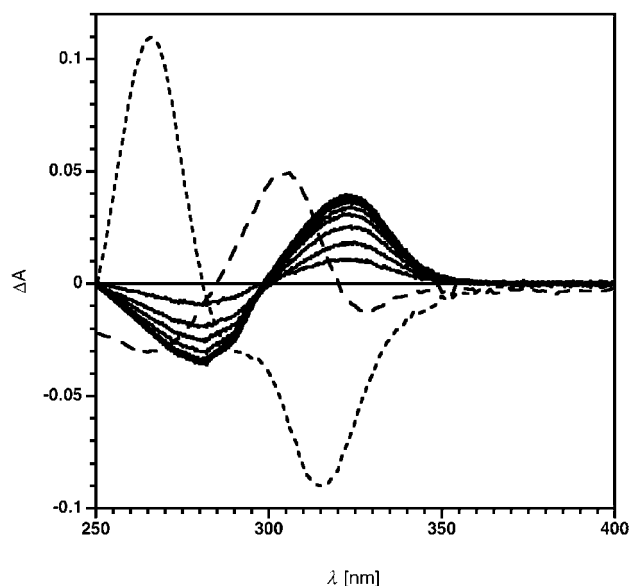


Fig. 2. Change in absorbance associated with the binding of $\text{CH}_3\text{-H}_4\text{Pte}(\text{Glu})_3$ to MetE. MetE ($10\ \mu\text{M}$) in AMT buffer (pH 7.0) was titrated with $2\text{-}\mu\text{M}$ aliquots of $\text{CH}_3\text{-H}_4\text{Pte}(\text{Glu})_3$ to a final concentration of $16\ \mu\text{M}$. The absorbances at $\lambda = 265$ and $320\ \text{nm}$ decreased and increased, resp., as the titration proceeded. The difference spectrum (---) was recorded for ($10\text{-}\mu\text{M}$ $\text{CH}_3\text{-H}_4$ folate in 80% MeCN/20% AMT buffer, pH 3) – ($10\text{-}\mu\text{M}$ $\text{CH}_3\text{-H}_4$ folate in AMT buffer, pH 7.2); the difference spectrum (---) was obtained for ($10\text{-}\mu\text{M}$ $\text{CH}_3\text{-H}_4$ folate in 80% MeCN/20% AMT buffer, pH 7.2) – ($10\text{-}\mu\text{M}$ $\text{CH}_3\text{-H}_4$ folate in AMT buffer, pH 7.2).

Fig. 2 shows a similar experiment performed with MetE at pH 7.0. Because MetE lacks any organic chromophore, these experiments can be performed with the full-length protein. Again, the binding of $\text{CH}_3\text{-H}_4$ folate is associated with an increased absorbance at $320\ \text{nm}$ and a decreased absorbance at $265\ \text{nm}$, indicating that protonation is not occurring. The K_D for $\text{CH}_3\text{-H}_4$ folate binding is independent of pH between 5.5 and 8.1, suggesting that protonation does not occur throughout the stability range of the protein.

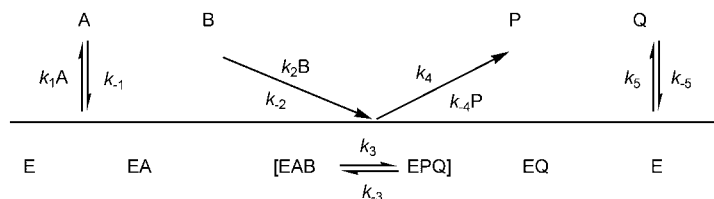
A potential alternative to activation of $\text{CH}_3\text{-H}_4$ folate by protonation would involve conversion of N(5) from an sp^3 to an sp^2 center by oxidation. However, if oxidation of the $\text{CH}_3\text{-H}_4$ folate cofactor had occurred in binary complexes with either MetE or MetH⁽²⁻⁶⁴⁹⁾, characteristic absorbance changes would have been detected in these titrations, which was not the case. Indeed, earlier studies by Taylor and Weissbach [17] had shown that tritium from $[6,7\text{-}^3\text{H}_2]\text{-5-CH}_3\text{-H}_4$ folate was not released to the solvent during the Me transfer to Hcy catalyzed by MetH, which indicates that $7,8\text{-H}_2\text{-5-CH}_3\text{-H}_4$ folate was not an intermediate. Competition experiments performed in the Arigoni group by Raillard [18] further demonstrated that there was no V/K isotope effect associated with tritium at C(6) of $\text{CH}_3\text{-H}_4$ folate.

Protonation Occurs In the Ternary Complex. Studies with both MetH⁽²⁻⁶⁴⁹⁾ and MetE suggest that protonation of $\text{CH}_3\text{-H}_4$ folate occurs only on formation of the ternary complex. In the case of MetH⁽²⁻⁶⁴⁹⁾, this ternary complex is formed when cob(I)alamin

binds to the $E \cdot \text{CH}_3\text{-H}_4\text{folate}$ binary complex, while the ternary complex in MetE is formed when Hcy binds to the $E \cdot \text{CH}_3\text{-H}_4\text{folate}$ binary complex.

The reaction of $\text{MetH}^{(2-649)}$ with exogenous cob(I)alamin is first order in both cobalamin cofactor and $\text{MetH}^{(2-649)}$, but exhibits saturation with $\text{CH}_3\text{-H}_4\text{folate}$, as shown in Fig. 3. Similarly, reaction of $\text{MetH}^{(2-649)}$ with methylcobalamin and H_4folate is first order in cobalamin and protein, and exhibits saturation with H_4folate (data not shown). These reactions can be described by the *Theorell–Chance* kinetic mechanism shown in Scheme 2, in which the ternary complex never accumulates during steady-state turnover.

Scheme 2. Theorell–Chance *Kinetic Mechanism for the Reaction of $\text{MetH}^{(2-649)}$ with Cob(I)alamin*. Here, ‘A’ represents $\text{CH}_3\text{-H}_4\text{folate}$, ‘B’ cob(I)alamin, ‘P’ methylcobalamin, and ‘Q’ H_4folate .



The net rate constants [19] for each step in the forward reaction are:

$$k'_5 = k_5 \quad ([Q] = 0) \quad (3)$$

$$k'_4 = k_4 \quad ([P] = 0) \quad (4)$$

$$k'_3 = \frac{k_3 k_4}{k_{-3} + k_4} \quad (5)$$

$$k'_2 = \frac{k_2 [B] k_3 k_4}{(k_{-3} + k_4) k_{-2} + k_3 k_4} \quad (6)$$

$$k'_1 = \frac{k_1 [A] k_2 [B] k_3 k_4}{k_{-1} k_{-3} k_{-2} + k_{-1} k_4 k_{-2} + k_{-1} k_3 k_4 + k_2 [B] k_3 k_4} \quad (7)$$

The velocity of the forward reaction is:

$$v_f = [E_T] / \left[\frac{1}{k'_1} + \frac{1}{k'_2} + \frac{1}{k'_3} + \frac{1}{k'_4} + \frac{1}{k'_5} \right] \quad (8)$$

Because all our measurements are conducted in the v/K_B regime at saturating A (that is to say, at unsaturating B, where the observed rate is first order in enzyme and cobalamin), this equation reduces to:

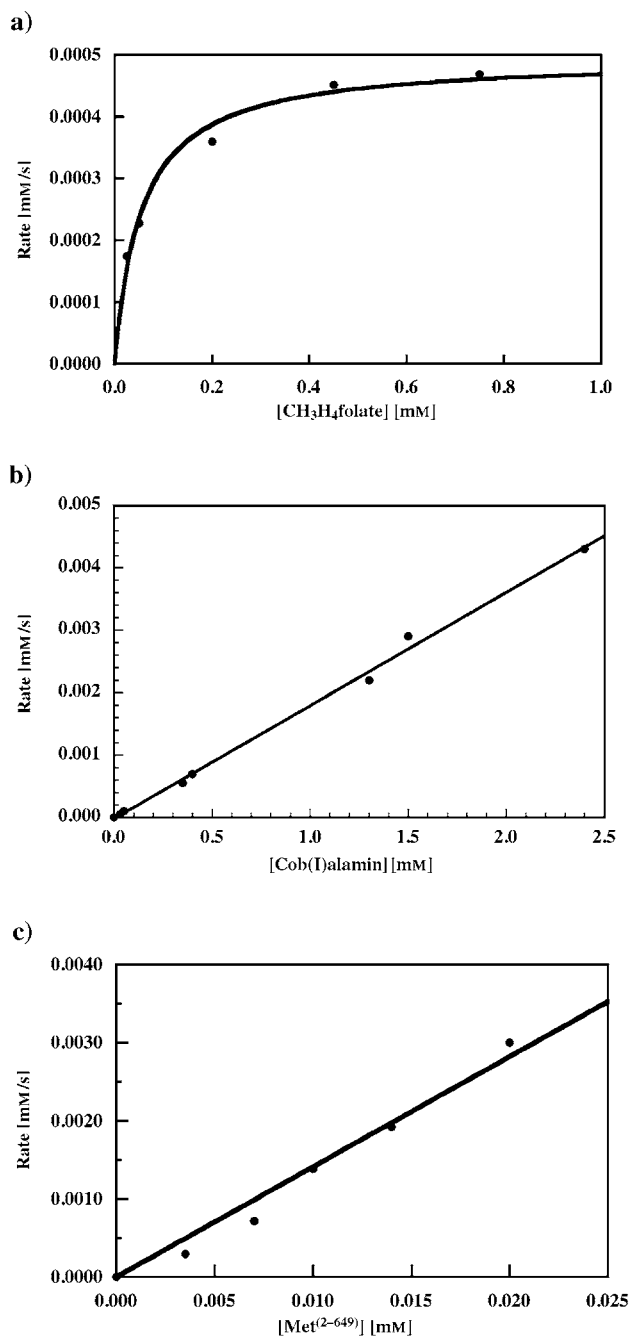


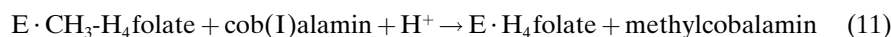
Fig. 3. Concentration dependence of the Me-transfer reaction mediated by CH₃-H₄folate-cob(I)alamin. The vertical axes represent the rate of methylcobalamin formation as a function of a) [CH₃-H₄folate] ([cob(I)alamin] = 0.3 mM, [enzyme] = 3.5 μM; data fit to a Michaelis–Menten binding equation, $K_M = 60 \pm 15$ μM); b) [cob(I)alamin] ([enzyme] = 3.5 μM, [CH₃-H₄folate] = 0.4 mM); c) [MetH⁽²⁻⁶⁴⁹⁾] ([cob(I)alamin] = 0.3 mM, [CH₃-H₄folate] = 0.4 mM). All experiments were performed in AMT buffer, pH 7.2, at 37°.

$$\frac{v_f}{[E_T]} = \frac{k'_2}{[B]} = \frac{k_2 k_3 k_4}{k_{-2} k_{-3} + k_{-2} k_4 + k_3 k_4} = \frac{k_2}{\frac{k_{-2}}{k_3} \left(\frac{k_{-3}}{k_4} + 1 \right) + 1} \quad (9)$$

In the reverse direction, assuming saturating Q , the equation is:

$$\frac{v_r}{[E_T]} = \frac{k'_{-4}}{[P]} = \frac{k_{-4} k_{-3} k_{-2}}{k_4 k_3 + k_4 k_{-2} + k_{-3} k_{-2}} = \frac{k_{-4}}{\frac{k_4}{k_{-3}} \left(\frac{k_{-3}}{k_{-2}} + 1 \right) + 1} \quad (10)$$

Thus, when A is saturating, v/K_B is not dependent on k_1 or k_5 , and when P is saturating, v/K_P is not dependent on k_{-5} or k_{-1} , but only on the rates of interconversion of EA and EQ. The overall reaction requires the uptake of a proton in the forward direction and release of a proton in the reverse direction, as shown in *Eqn. 11*.



A kinetic analysis of the pH dependence of the $\text{CH}_3\text{-H}_4\text{folate-cob(I)alamin}$ and $\text{methylcobalamin-H}_4\text{folate}$ methyltransferase activities of $\text{MethH}^{(2-649)}$ is shown in *Fig. 4*. In the presence of saturating $\text{CH}_3\text{-H}_4\text{folate}$, the second-order rate constant for the formation of cob(I)alamin increases from a value of *ca.* $100 \text{ M}^{-1}\text{s}^{-1}$ at pH 9 to an estimated value of $9,000 \text{ M}^{-1}\text{s}^{-1}$ at low pH. The reverse reaction shows an opposite trend, with the plateau value at high pH being $95 \text{ M}^{-1}\text{s}^{-1}$. These kinetics indicate that the pH dependence arises during the interconversion of EA ($E \cdot \text{CH}_3\text{-H}_4\text{folate}$) and EP ($E \cdot \text{H}_4\text{folate}$), *i.e.*, in the ternary complex prior to or associated

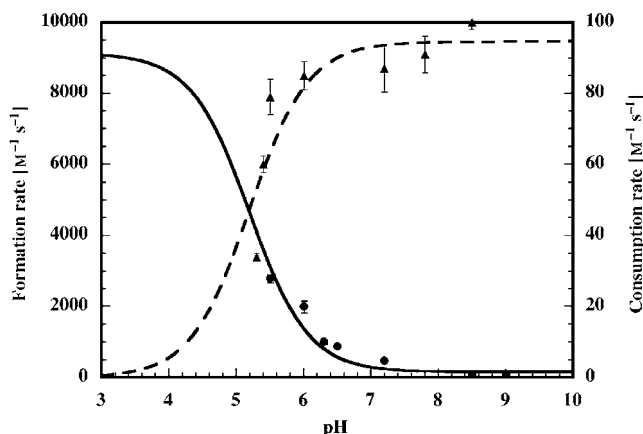
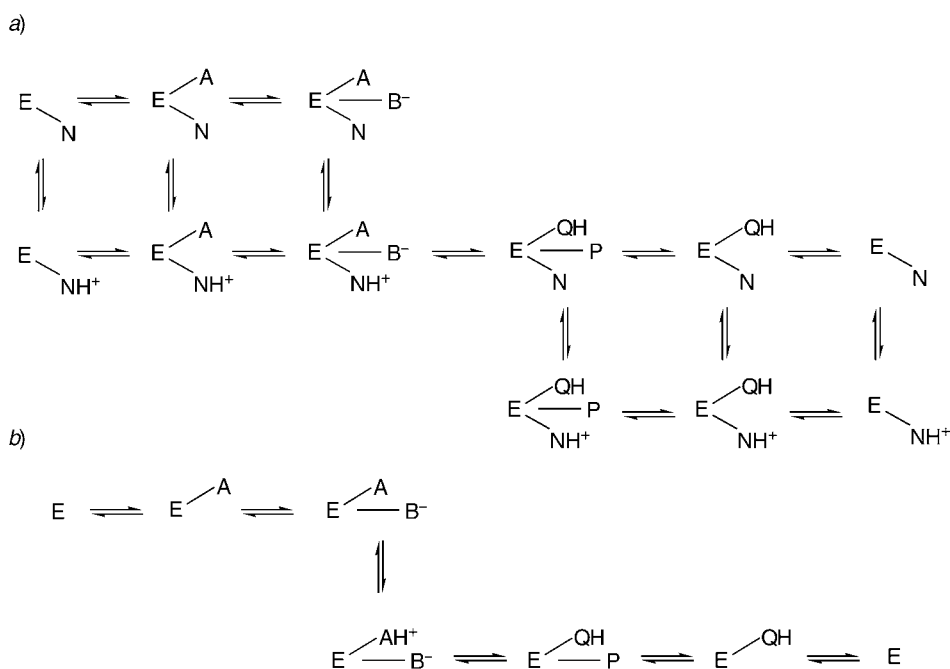


Fig. 4. pH Dependence of Me-transfer reactions. Each data point represents the maximum rate constant determined from plots of velocity vs. $[\text{CH}_3\text{-H}_4\text{folate}]$ or $[\text{H}_4\text{folate}]$ at the pH indicated. The error bars represent the error in the *Michaelis-Menten* curve fit. Solid triangles (\blacktriangle) refer to the $\text{H}_4\text{folate-methylcobalamin}$, filled circles (\bullet) to the $\text{CH}_3\text{-H}_4\text{folate-cob(I)alamin}$ Me-transfer reactions. To fit the data (see *Exper. Part*), we assumed an apparent $\text{p}K_a$ of 5.3, without including set end points for the curves.

with the release of the first product. The pH-dependent rate profiles do not tell us whether the proton is bound to $\text{CH}_3\text{-H}_4\text{folate}$ or to a general-acid catalyst on the enzyme.

The pH dependence observed in the forward and reverse directions is consistent with either of the plausible mechanisms shown in *Scheme 3*. In *Scheme 3,a*, the pH-dependence reflects the protonation of a general-acid/base catalyst on the enzyme that must be protonated for reaction of $\text{CH}_3\text{-H}_4\text{folate}$ with cob(I)alamin and deprotonated for reaction of H_4folate with methylcobalamin. In *Scheme 3,b*, protonation occurs directly on $\text{CH}_3\text{-H}_4\text{folate}$ in the ternary complex, without the necessity for any general-acid catalyst on the enzyme.

Scheme 3. Alternate Mechanisms for MetH Catalysis Involving a) General-Acid/Base Catalysis by a Residue on the Protein or b) by Protonation of $\text{CH}_3\text{-H}_4\text{Folate}$ in the Ternary Complex (which does not require the participation of a general-acid/base catalyst on the enzyme). Both mechanisms are consistent with the pH-rate profiles given in Fig. 4. Designations: N = general-acid/base catalyst on the enzyme, A = $\text{CH}_3\text{-H}_4\text{folate}$, QH = H_4folate , B^- = cob(I)alamin anion, P = methylcobalamin.



Preliminary pre-steady-state experiments performed with MetE (unpublished data) suggest that protonation of $\text{CH}_3\text{-H}_4\text{folate}$ also requires formation of a ternary $\text{E} \cdot \text{CH}_3\text{-H}_4\text{folate} \cdot \text{Hcy}$ complex. In this case, protonation occurs at a rate faster than the rate of Me transfer from $\text{CH}_3\text{-H}_4\text{folate}$ to Hcy, and the $\text{p}K_a$ of $\text{CH}_3\text{-H}_4\text{folate}$ in the ternary complex is sufficiently high that most of the enzyme-bound $\text{CH}_3\text{-H}_4\text{folate}$ is protonated at pH 7.2.

Structural Data of Homologues of the Substrate-Binding Domains of Cobalamin-Dependent Methionine Synthase. – As already mentioned, betaine–homocysteine methyltransferase (BHMT) shows significant sequence homology to the Hcy-binding module of MetH. The structure of BHMT was determined recently [20]. The enzyme corresponds to a $\beta_8\alpha_8$ barrel of the general form observed in triose phosphate isomerase. The essential Zn ion is secured within the barrel by three conserved Cys ligands: Cys²¹⁷, Cys²⁹⁹, and Cys³⁰⁰ in human BHMT. The barrel is distorted to accommodate the Zn binding site: Cys²¹⁷ is at the C-terminus of strand β_6 , and Cys²⁹⁹ and Cys³⁰⁰ are at the C-terminus of strand β_8 . In an undistorted barrel, the side chains of the three Cys residues would be too far apart to be bridged by a Zn ion, but in BHMT, strand β_7 is extruded from the barrel, allowing β_6 and β_8 to move closer together. The fourth ligand to the Zn-atom in BHMT is presumed to be a H₂O molecule.

The BHMT structure has also been investigated with a transition-state analogue, (S)-(δ -carboxybutyl)-L-Hcy, bound at the active site. This compound can be viewed as a ‘bi-substrate’ analogue. Its S-atom is ligated to Zn, which displays tetrahedral coordination to four sulfur ligands. The conserved residue Glu¹⁵⁹ on strand β_4 reaches across the barrel to form a H-bond with the amino group of the Hcy moiety, presumably stabilizing its protonated form, and the O-atoms of the Hcy carboxylate group are H-bonded to backbone amide groups just beyond the end of strand β_1 . To accommodate this interaction with substrate, strands β_1 and β_2 are splayed apart by interposition of a H-bond between the carboxylate of Asp²⁶ on β_1 and a backbone amide on β_2 . The binding site is flagged by a Asp-Gly-Gly/Ala motif, in which the small residues are critical to allow H-bonding to the peptide backbone.

Although many enzymes contain $\beta_8\alpha_8$ barrels, the particular distortions found in BHMT make this barrel distinctive. The program DALI [21] can be used to search the structural data in the protein data bank (PDB) for similarly distorted barrels [20]. A closely related structure is that of uroporphyrin decarboxylase, which has a similar cleft between strands β_1 and β_2 , formed, in this case, by H-bonding between a conserved Gln side chain and a backbone NH in strand β_2 . Fig. 5 Shows an overlay of uroporphyrin

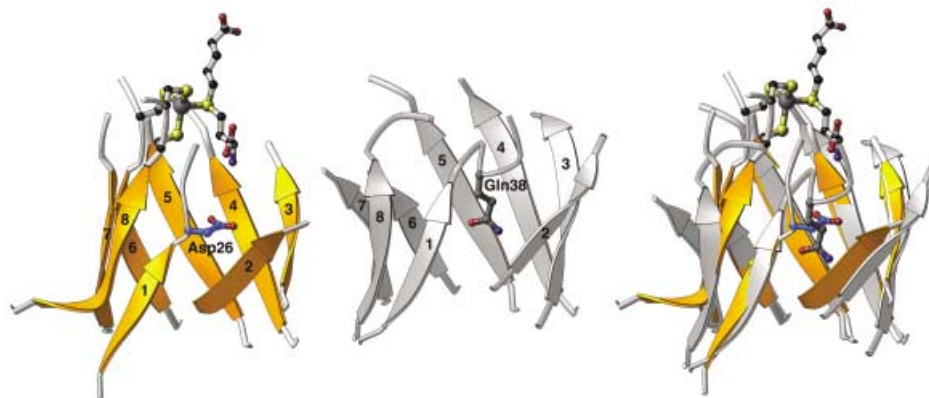


Fig. 5. Structures of betaine–homocysteine methyltransferase (left, gold), uroporphyrin decarboxylase (center, silver), and their superposition (right). In BHMT, the cleft between strands 1 and 2 is generated by the side chain of Asp²⁶; Gln³⁸ occupies an analogous position in the structure of UroD.

decarboxylase and BHMT to illustrate the similar structural features of these two barrels, despite a lack of any detectable sequence similarity. Uroporphyrin decarboxylase does not contain a metal cofactor, but in the UroD barrel, strands $\beta 6$ and $\beta 7$ have been extruded, which brings strands $\beta 5$ and $\beta 8$ close to one another.

Uroporphyrin decarboxylase does show significant sequence similarity with two related methylcobamide methyltransferases, MT2-A and MT2-M, also known as MtbA and MtaA [22]. These two proteins catalyze the Me transfer from methylcobamide to coenzyme M (2-mercaptoethanesulfonic acid), reactions that are similar to the methylcobalamin-Hcy methyltransferase reaction catalyzed by MetH. They contain Zn ions to coordinate the sulfido group of coenzyme M [23][24], and these Zn ions are bound by two Cys and a His [24]. His²³⁹Asn, Cys²⁴¹Ser, and Cys³¹⁶Ser (numbering for MT2-M) mutants display complete or nearly complete loss of activity, which suggests that they are the ligated to Zn in both MT2-A and MT2-M [24]. Although there is no significant sequence similarity between MetE and MT2-A or MT2-M, the nature of the Zn ligands and their relative locations in the sequences are strikingly similar, which suggests that the MetE and MT2 families exhibit structural similarities. Alignment of the sequence of MT2-M with that of uroporphyrin decarboxylase places the GlyCys³¹⁶Gly sequence of the downstream Cys ligand at the C-terminal end of strand $\beta 8$, in roughly the position of the GlyCys²⁹⁹Cys³⁰⁰ sequence of BHMT. The upstream His²³⁹IleCys²⁴¹ sequence maps onto strand $\beta 5$. In Fig. 6, we have grafted the Zn ligands

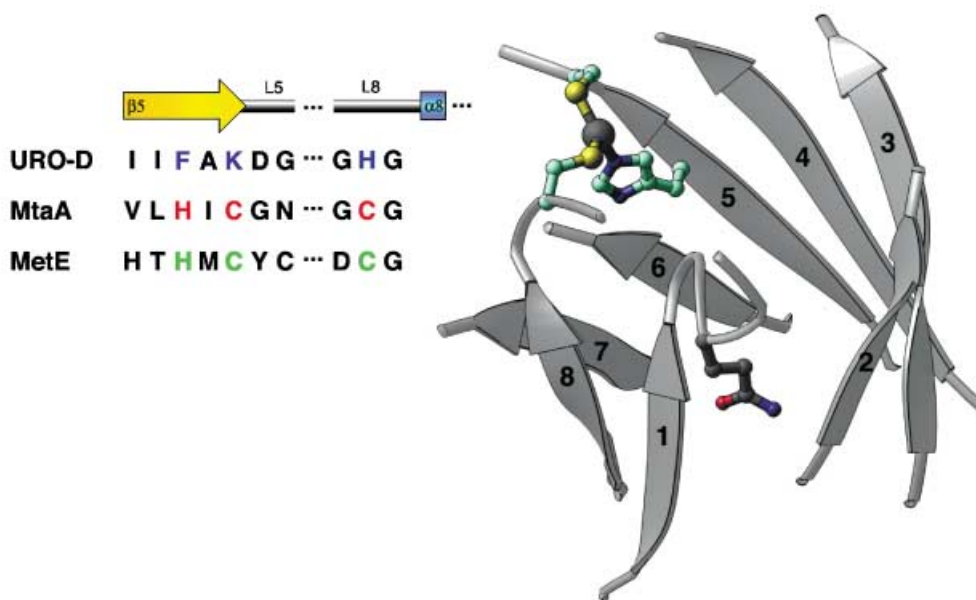


Fig. 6. Model of the metal-binding site of MetE. The structure was generated on the basis of the coordinates of UroD. Based on the alignment of UroD with MT2-M (MtaA), gaps in the sequence alignment from ClustalW were adjusted to allow His²³⁹ and Cys²⁴¹ to point toward the center of the barrel. Residues (in green) coordinating the Zn-atom, which was added without distorting the backbone geometry of UroD, were modeled by the following simulated mutations: Phe²⁶¹ → His, Lys²⁶³ → Cys, and His³³⁹ → Cys.

of MT2-M onto the structure of uroporphyrin decarboxylase to create a model for the Zn-binding site in MetE.

The connections between UroD and BHMT on the one hand, and MT2-A and MetE on the other, suggest that the architecture of the Hcy-binding sites of MetE and MetH will be strikingly similar, despite the lack of sequence similarity and the differences in ligands and ligand spacing. Perhaps, there is not more than one way to skin a cat! In this context, it should be noted that in Archaea, MetE sequences specify *ca.* 34-kDa proteins that are only half of the length of the corresponding sequences in eukaryotes and eubacteria, and align with the C-terminal half of the larger proteins. The Zn ligands are contained in this half of the protein and are conserved in Archaea. The MetE protein from *Methanobacterium thermoautotrophicum* has been purified and shown to catalyze Me transfer from methylcobalamin to Hcy [25]. This enzyme does not use CH₃-H₄folate or methyltetrahydromethanopterin as a Me donor. Thus, the Hcy-binding domain of MetE can be adapted to accommodate methylcobalamin as a Me donor, which further strengthens the picture that the chemical strategies for activation of Hcy are highly similar.

The CH₃-H₄folate-binding module of cobalamin-dependent methionine synthase is also homologous to a protein that has been structurally characterized, the AcsE subunit of the acetyl CoA synthase from *Moorella (Clostridium) thermoacetium*. AcsE catalyzes the Me transfer from CH₃-H₄folate to the corrinoid cofactor of another subunit in the synthase complex, the corrinoid iron–sulfur protein. The methyltransferase shows significant sequence similarity to residues 353–623 of MetH [26], which constitute the CH₃-H₄folate-binding module of MetH. The pH-rate profiles obtained for the activities of CH₃-H₄folate–cob(I)alamin and H₄folate–methylcobalamin methyltransferase catalyzed by AcsE [27] are very similar to those shown for MetH in Fig. 4, so, the mechanism for this Me transfer is likely to be very similar, too.

The structure of AcsE has been determined [28]. This protein is also a β₈α₈ barrel, with the binding site for CH₃-H₄folate straddling the C-termini of the barrel strands. A model of CH₃-H₄folate was built into the binding site, and positioned to form H-bonding interactions with three conserved Asp and two Asn residues. The most-surprising feature of this structure is the absence of any general-acid/base catalysts near N(5) of CH₃-H₄folate. The conserved residue Asn¹⁹⁹ lies above N(5) and O(4) of the pterin ring, but Asn is not expected to serve as a general-acid/base catalyst. The absence of a suitable catalytic group leads us to favor the mechanism shown in Scheme 3,b, in which protonation of enzyme-bound CH₃-H₄folate in the ternary complex does not involve the intervention of a residue on the enzyme. In this mechanism, the protonation of N(5) of CH₃-H₄folate bound in a hydrophobic environment occurs only when the electron-rich corrin ring of cob(I)alamin is juxtaposed to provide charge compensation. The resultant Me transfer by an S_N2 mechanism dissipates the charge, and the reaction is favored by the low dielectric constant in the desolvated ternary complex.

The strategy employed by MetE may be quite similar. CH₃-H₄folate is introduced into an apolar environment on binding to the enzyme, and protonation occurs only when ternary-complex formation introduces an electron-rich Zn–S moiety into the vicinity. The apolar environment may then facilitate reaction to dissipate the charge pair. Thus, the mechanisms for activation of CH₃-H₄folate in the ‘improbable’ and ‘impossible’ reactions may indeed be almost identical.

Experimental Part

Materials. MetH⁽²⁻⁶⁴⁹⁾ [8] and MetE [7] were prepared as previously described. L-Hcy was prepared by hydrolysis of L-homocysteine thiolactone (*Sigma Chemicals*, St. Louis, MO) [29]. AMT Buffer (50-mM AcOH, 50-mM 2-(*N*-morpholino)ethanesulfonic acid (MES), 100-mM triethanolamine) was adjusted to the appropriate pH with NaOH [30]. Super-reducing Ti^{III} citrate was prepared from TiCl₃ (*Aldrich*) [31].

Binding of L-Hcy to MetH⁽²⁻⁶⁴⁹⁾. Titrations were performed in a *Varian Cary-300* spectrophotometer fitted with both reference- and sample-cell holders. Split-cell quartz cuvettes (1-ml capacity per side, 0.4-cm path length per compartment) were placed in each sample chamber. A stirring bar was placed in each chamber to facilitate mixing during titration. One chamber in each cuvette was filled with MetH⁽²⁻⁶⁴⁹⁾ in buffer at the desired pH, while the second chamber contained an equal volume of buffer. A stock soln. of L-Hcy in 10-mM potassium phosphate buffer, pH 7.2, was added to the enzyme-containing compartment of the sample cuvette and to the buffer-containing compartment of the reference cuvette. An equal volume of 10-mM potassium phosphate buffer, pH 7.2, was added to the buffer-containing compartment of the sample cuvette and to the enzyme-containing compartment of the reference cuvette. The acquired UV/VIS spectra were corrected for dilution by the titrant, and for baseline drift, prior to plotting the absorbance at 236 nm vs. the concentration of L-Hcy. For each buffer system, the total molar absorbance change at high pH, where binding of L-Hcy to MetH⁽²⁻⁶⁴⁹⁾ was nearly stoichiometric, was used to calculate the concentration of the Zn–thiolate complex in all other titrations conducted in that buffer system. At lower pH, where higher concentrations of Hcy were needed, artifacts introduced by high absorbances precluded the use of concentrations of L-Hcy above 0.5 mM, preventing titration to saturation. The K_D value for the binding of L-Hcy to the active-site Zn of MetH⁽²⁻⁶⁴⁹⁾ was obtained by fitting the data to Eqn. 12 [32] using the KaleidaGraph program (*Synergy Software*).

$$[E_{\text{Zn-thiolate}}] = \frac{(E_T + [\text{L-Hcy}] + K_D) - \sqrt{(E_T + [\text{L-Hcy}] + K_D)^2 - 4E_T[\text{L-Hcy}]}}{2} \quad (12)$$

Release of protons associated with the binding of Hcy to MetE was measured by titration in a weakly buffered soln. containing phenol red, as described initially for experiments performed with MetH [13]. The enzyme (20 μM) was placed in 50-μM phosphate buffer, pH 7.2, containing 40-μM phenol red and 100-mM KCl, and titrated with 10-mM NaOH to determine a stoichiometry conversion factor of $\Delta A_{558}/\Delta H^+$. The enzyme was then titrated with a 2-mM stock soln. of Hcy in 50-μM phosphate buffer, containing 40-μM phenol red, adjusted to the same pH, and spectra were recorded after each addition. After correcting for dilution, use of the conversion factor $\Delta A_{558}/\Delta H^+$ allowed construction of a binding curve for Hcy.

Absorbance Change Associated with the Binding of CH₃-H₄Pte(Glu)₃ to MetE. The difference titration of MetE (20 μM) was performed at 25° in AMT buffer/10-mM potassium phosphate, adjusted to pH 7.0 with NaOH. Titrations were performed using split-cell quartz cuvettes in a *Varian Cary-300* spectrophotometer fitted with a single-reference and sample-cell holder as described in the preceding paragraph. A 2-mM soln. of CH₃-H₄Pte(Glu)₃ in AMT buffer/10-mM potassium phosphate, pH 7.0, was added to MetE in the front compartment of the sample cuvette and to the buffer in the rear compartment of the reference cuvette, while an equal volume of buffer was added to the rear compartment of the sample cuvette and to the front compartment of the reference cuvette. Difference spectra were corrected for dilution before plotted.

Activities of CH₃-H₄folate–Cob(I)alamin and H₄folate–Methylcobalamin Methyltransferase Catalyzed by MetH⁽²⁻⁶⁴⁹⁾. All reactions were conducted at 37°. MetH⁽²⁻⁶⁴⁹⁾ (20 μM in AMT buffer at the desired pH, containing 400-μM hydroxocob(III)alamin) was placed in an O₂-free cuvette equipped with a sidearm and a rubber septum. Then, CH₃-H₄folate, sufficient for a final conc. of 10 μM to 1 mM, was placed in the sidearm, and the mixture was degassed by repeated equilibration with Ar gas followed by evacuation. Ti^{III} citrate (4-mM final conc.) was added through the septum with a gas-tight syringe, and the cuvette was incubated for 10 min at 37°. The reaction was initiated by tipping in the CH₃-H₄folate from the side arm and was followed by measuring the change in absorbance at λ = 538 nm (formation of methylcobalamin). At pH 5.5–6.9, where reduction of hydroxocob(III)alamin by Ti^{III} is not optimal, a conc. stock soln. of hydroxocob(III)alamin, reduced with Ti^{III} citrate to cob(I)alamin, was prepared in AMT buffer, pH 7.2, and was transferred to the assay cuvette with a gas-tight syringe inserted through the rubber septum. The small volume (40 μl) of pH 7.2 AMT buffer did not alter the pH of the assay soln. (1-ml final volume). The H₄-folate–methylcobalamin methyltransferase assay was performed as described previously [33], using MetH⁽²⁻⁶⁴⁹⁾ in AMT buffer adjusted to the desired pH. At each pH value, the reaction rate was measured as a function of the concentration of the folate substrate, and the maximum velocity

was obtained by fitting the data to the *Michaelis–Menten* equation [32] shown in *Eqn. 13*, where ‘S’ is the folate substrate.

$$\frac{v}{v_{\max}} = \frac{[S]}{K_s + [S]} \quad (13)$$

The dependence of the CH₃-H₄folate–cob(I)alamin-methyltransferase reaction on the concentration of cob(I)alamin was examined at pH 7.2, and at pH 9.0, where the reaction is slowest; the dependence of the reaction on methylcobalamin concentration was determined at pH 7.2 and at pH 5.5, where the reaction is slowest. The data of the pH-rate profiles were fit to *Eqn. 14* using the KaleidoGraph software, fixing the pK_a at 5.3. The values for v_{max} and v_{min} (the maximal velocities at the pH extremes) were determined by successive iterations.

$$v_{\max}^{\text{app}} = \frac{v_{\max} + (v_{\min} \times 10^{(\text{pH}-\text{pK}_a)})}{1 + 10^{(\text{pH}-\text{pK}_a)}} \quad (14)$$

REFERENCES

- [1] A. E. Smith, R. G. Matthews, *Biochemistry* **2000**, *39*, 13880.
- [2] R. E. Benesch, R. Benesch, *J. Am. Chem. Soc.* **1955**, *77*, 5877.
- [3] J. C. González, R. M. Banerjee, S. Huang, J. S. Sumner, R. G. Matthews, *Biochemistry* **1992**, *31*, 6045.
- [4] J. C. González, K. Peariso, J. E. Penner-Hahn, R. G. Matthews, *Biochemistry* **1996**, *35*, 12228.
- [5] Z. S. Zhou, A. E. Smith, R. G. Matthews, *Bioorg. Med. Chem. Lett.* **2000**, *10*, 2471.
- [6] K. Peariso, Z. S. Zhou, A. E. Smith, R. G. Matthews, J. E. Penner-Hahn, *Biochemistry* **2001**, *40*, 987.
- [7] Z. S. Zhou, K. Peariso, J. E. Penner-Hahn, R. G. Matthews, *Biochemistry* **1999**, *38*, 15915.
- [8] C. W. Goulding, D. Postigo, R. G. Matthews, *Biochemistry* **1997**, *50*, 8052.
- [9] T. A. Garrow, *Biochemistry* **1996**, *37*, 22831.
- [10] C. W. Goulding, R. G. Matthews, *Biochemistry* **1997**, *36*, 15749.
- [11] K. Peariso, C. W. Goulding, S. Huang, R. G. Matthews, J. E. Penner-Hahn, *J. Am. Chem. Soc.* **1998**, *120*, 8410.
- [12] A. P. Breksa III, T. A. Garrow, *Biochemistry* **1999**, *38*, 13991.
- [13] J. T. Jarrett, C. Y. Choi, R. G. Matthews, *Biochemistry* **1997**, *36*, 15739.
- [14] M. Vasák, H. R. Kägi, H. A. O. Hill, *Biochemistry* **1981**, *20*, 2852.
- [15] D. B. Rozema, C. D. Poulter, *Biochemistry* **1999**, *38*, 13138.
- [16] J. J. Wilker, S. Lippard, *Inorg. Chem.* **1997**, *36*, 969.
- [17] R. T. Taylor, H. Weissbach, *Arch. Biochem. Biophys.* **1968**, *123*, 109.
- [18] S. Raillard, Ph.D. thesis, Eidgenössische Technische Hochschule, Zürich, 1991.
- [19] W. W. Cleland, *Biochemistry* **1975**, *14*, 3220.
- [20] J. C. Evans, D. P. Huddler, J. Jiracek, C. Castro, N. S. Millian, T. A. Garrow, M. L. Ludwig, *Structure* **2002**, *10*, 1159.
- [21] L. Holm, C. Sander, *Nucleic Acids Res.* **1997**, *25*, 231.
- [22] U. Harms, R. K. Thauer, *Eur. J. Biochem.* **1996**, *235*, 653; L. Paul, J. A. Krzycki, *J. Bacteriol.* **1996**, *178*, 6599.
- [23] G. M. LeClerc, D. Grahame, *J. Biol. Chem.* **1996**, *271*, 18725.
- [24] S. Gencic, G. M. LeClerc, N. Gorlatova, K. Peariso, J. E. Penner-Hahn, D. Grahame, *Biochemistry* **2001**, *40*, 13068.
- [25] I. Schröder, R. K. Thauer, *Eur. J. Biochem.* **1999**, *263*, 789.
- [26] D. L. Roberts, S. Zhao, T. Doukov, S. W. Ragsdale, *J. Bacteriol.* **1994**, *176*, 6127.
- [27] S. Zhao, D. L. Roberts, S. W. Ragsdale, *Biochemistry* **1995**, *34*, 15075.
- [28] T. Doukov, J. Seravalli, J. J. Stezowski, S. W. Ragsdale, *Structure* **2000**, *8*, 817.
- [29] J. T. Drummond, J. T. Jarrett, J. C. González, S. Huang, R. G. Matthews, *Anal. Biochem.* **1995**, *228*, 323.
- [30] K. J. Ellis, J. F. Morrison, *Methods Enzymol.* **1982**, *87*, 405.
- [31] B. Bhaskar, E. DeMoll, D. Grahame, *Biochemistry* **1998**, *37*, 14491.
- [32] I. H. Segel, ‘Enzyme Kinetics: Behavior and Analysis of Rapid Equilibrium and Steady-State Enzyme Systems’, John Wiley & Sons, New York, 1975.
- [33] J. T. Jarrett, C. W. Goulding, K. Fluhr, S. Huang, R. G. Matthews, *Methods Enzymol.* **1997**, *281*, 196.

Received August 25, 2003